



Alaa E. Fayed, Peter L. Nesper, and Amani A. Fawzi

## Anatomy of the Retinal Vascular System

The retina is supplied by two circulations: the choroidal circulation via the choroidal vessels and the retinal circulation via the central retinal artery (Jakobiec 1982). In up to 32% of the eyes (Justice and Lehmann 1976), an additional branch, the cilioretinal artery, may extend from the choroidal circulation to supply a portion of the inner retina, mainly in the macular region.

The choroidal circulation is supplied by the ophthalmic artery via the medial and lateral posterior ciliary arteries, each of which gives rise to one long and multiple short posterior ciliary arteries. Apart from minor contributions from recurrent branches of the long posterior ciliary arteries, the choriocapillaris is supplied by the short posterior arteries, which penetrate the posterior globe near the optic nerve (Oyster 1999). Paula et al. demonstrated that there is a higher arteriolar supply from the posterior ciliary artery surrounding the macula than the rest of the retina, with approximately nine pairs of arterioles and venules distributed in the parafoveal regions (Paula et al. 2010).

It was previously thought that branches from the central retinal vessels form only two distinct capillary beds, one in the nerve fiber layer (superficial capillary plexus or SCP) and the other in the deep boundary between the inner nuclear layer and the outer plexiform layer (deep capillary plexus or DCP) (Grant and Luttly 2012). Until recently, the visualization of these capillary systems remained inaccessible except via fluorescein angiography (FA). Weinhaus et al. reported that the SCP was visualized over four times more effectively than the DCP in FA, thereby limiting the under-

standing of the vascular pathology affecting these deeper layers (Weinhaus et al. 1995).

The development of optical coherence tomography angiography (OCTA) allowed visualization of the deeper capillaries with sufficient detail to evaluate the impact of various vascular disorders at this level. Park et al. utilized OCTA to distinguish a middle capillary plexus (MCP) from the SCP and DCP which lies at the inner boundary of the inner nuclear layer (Park et al. 2016) (Fig. 11.1). Around the optic nerve, an additional fourth, more superficial capillary network, the radial peripapillary capillaries, exists (Max Snodderly and Weinhaus 1990).

## Fluorescein Angiography and Wide-Angle Imaging in Retinal Vascular Disease

### Diabetic Retinopathy

Retinal capillary microaneurysms develop as a saccular out-pouching from the capillary wall (Akram et al. 2013) and are readily detected in the early frames of FA where they appear as small hyperfluorescent dots. They may also show variable leakage which fades in the later frames. FA helps distinguish them from clinically similar tiny punctate dot hemorrhages that will generally block fluorescence (de Venecia et al. 1976) (Fig. 11.2).

Intraretinal microvascular abnormalities (IRMA) is a term used to describe clusters of abnormal hypercellular vascular structures that arise on the edges of areas of retinal capillary non-perfusion (Davis et al. 1968). Clinically, it can be difficult to distinguish IRMA from neovascularization (NV). On FA, IRMAs typically do not show leakage whereas NV does (Fig. 11.3).

In DR, distortion and enlargement of the foveal avascular zone (FAZ) result from occlusion of retinal capillaries and loss of precapillary arterioles near the fovea (Fig. 11.4). This was extensively documented by Conrath et al. (2005), Arend et al. (1995) and Bresnick et al. (1984). However, areas of

A. E. Fayed  
Department of Ophthalmology, Feinberg School of Medicine,  
Northwestern University, Chicago, IL, USA

Department of Ophthalmology, Kasr Al-Ainy School of Medicine,  
Cairo University, Giza, Egypt

P. L. Nesper · A. A. Fawzi (✉)  
Department of Ophthalmology, Feinberg School of Medicine,  
Northwestern University, Chicago, IL, USA

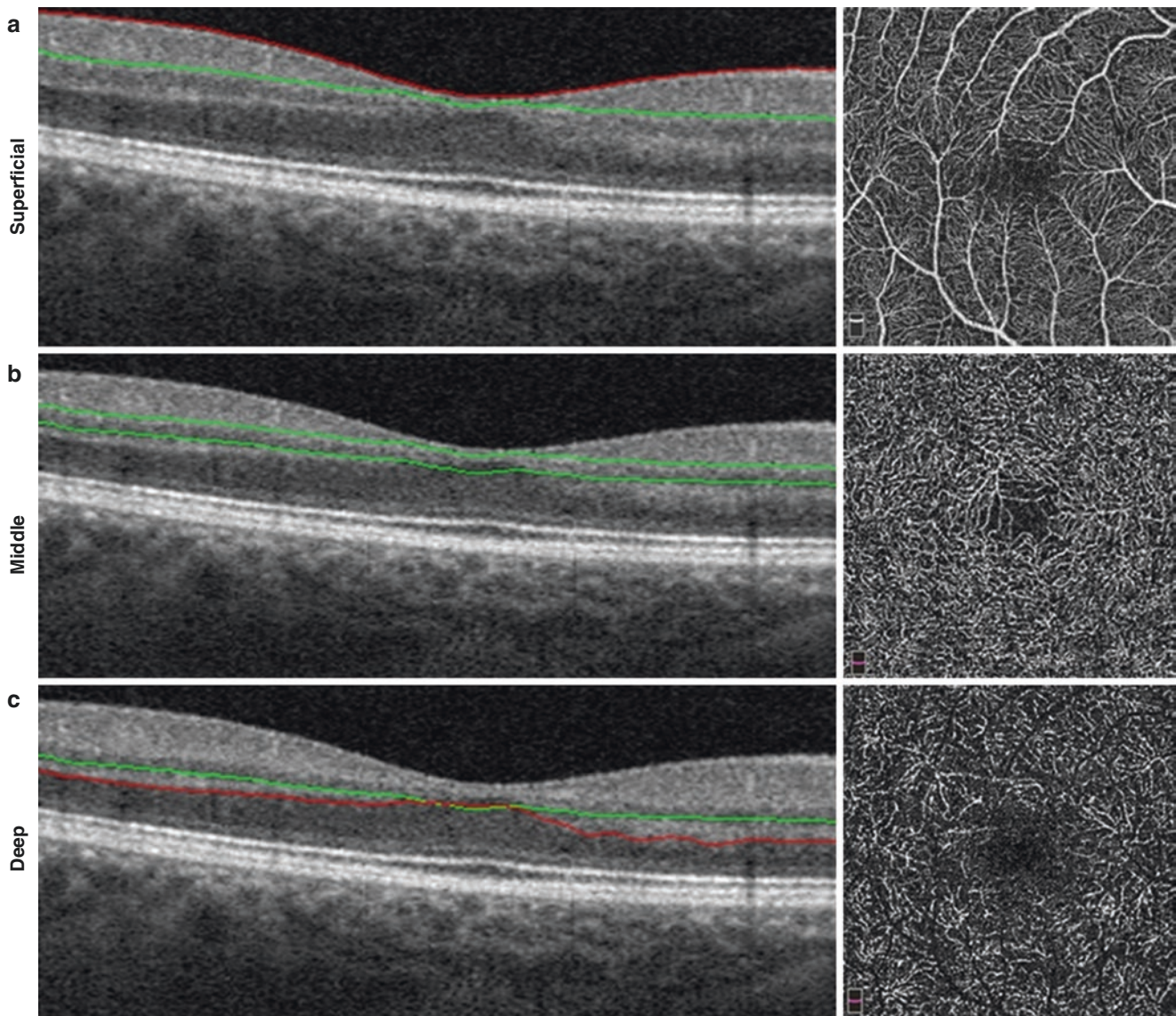


**Fig. 11.1** The three retinal capillary plexuses. Optical coherence tomography angiography segmentation using 3D projection artifact resolution (3D PAR) to visualize the three capillary plexuses. (a) The SCP boundaries encompass the nerve fiber layer and the ganglion cell layer (GCL), with a lower boundary set at 10  $\mu\text{m}$  above the IPL. (b) The

MCP was captured with a 40- $\mu\text{m}$  slab to encompass the inner boundary of the INL with an upper boundary set 10  $\mu\text{m}$  above the IPL and a lower boundary set 30  $\mu\text{m}$  below it. (c) The DCP was set to encompass the OPL and deep boundary of the INL, with an upper boundary set 30  $\mu\text{m}$  below the IPL and a lower boundary at 10  $\mu\text{m}$  below the OPL.

non-perfusion may be underappreciated on FA because of the diffuse leakage from surrounding vessels, especially in later frames.

Proliferative diabetic retinopathy (PDR) is characterized by the development of neovascularization at or around the disc (NVD) or surrounding areas of ischemia in the periphery, referred to as neovascularization elsewhere (NVE). NVD and NVE appear hyperfluorescent and tend to exhibit leakage on FA and wide field imaging (Figs. 11.5 and 11.6).

Diabetic macular edema (DME) is characterized by macular thickening caused by leakage from hyperpermeable vas-

culature (Wilkinson et al. 2003). It can be appreciated by FA as leaking of the dye in early frames, typically in a petalloid or honeycomb pattern (Otani and Kishi 2007) (Fig. 11.7). Borders of edematous retinal tissue may show waxy yellowish deposits, known as hard exudates. They form as a result of leakage of lipoprotein and fluid from damaged capillaries into the extracellular space of the retina (Ferris and Patz 1984). Increased amounts of hard exudate within the 30° photographic field centered on the macula has been associated with a higher risk of visual impairment (Chew et al. 1996).



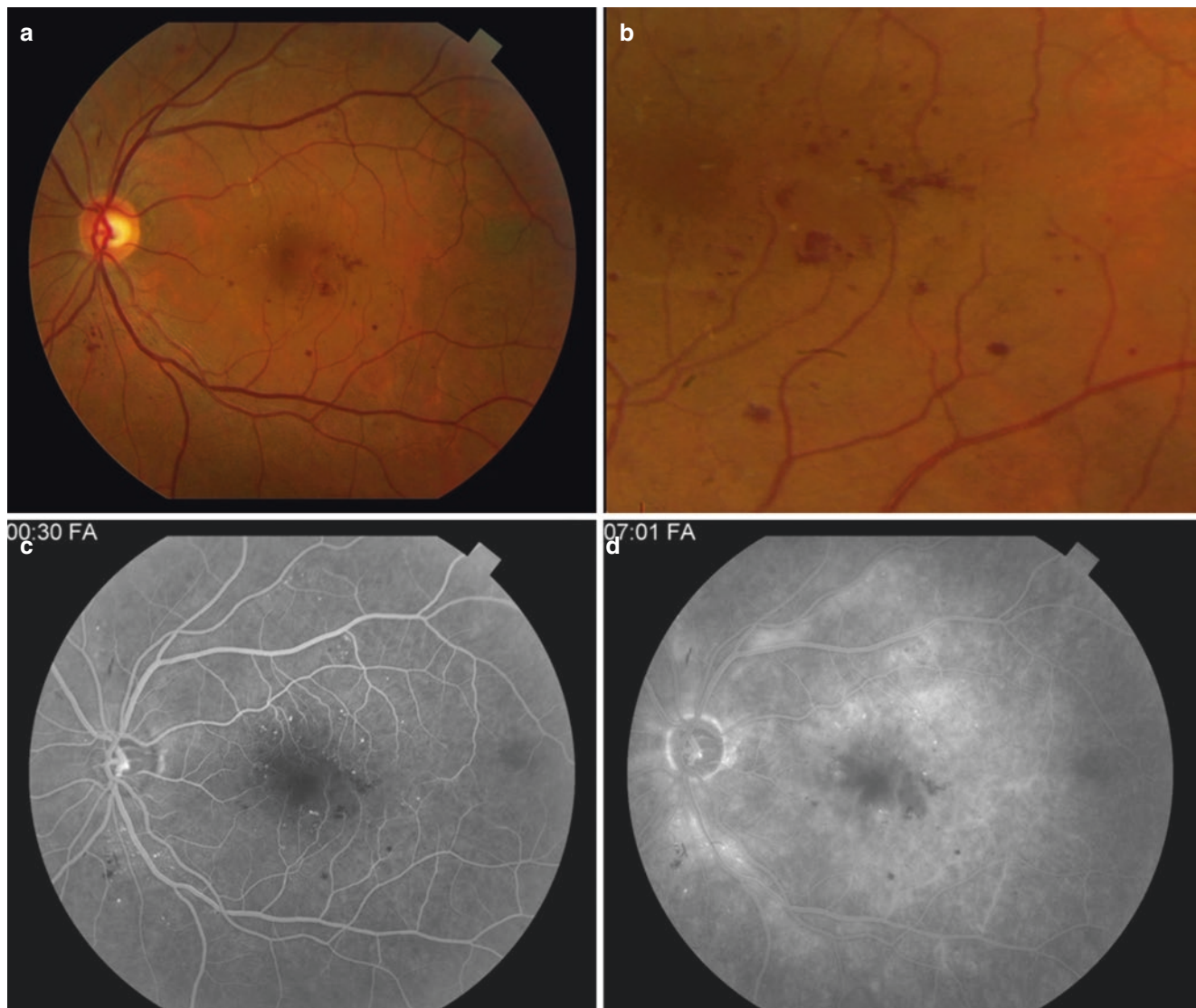


**Fig. 11.2** Microaneurysms in NPDR. (a) Fundus photo of the left eye showing multiple scattered microaneurysms throughout the posterior pole. (b) Scattered microaneurysms inferior and temporal to the fovea. (c) Fluorescein angiogram of the left eye during the late venous phase showing multiple scattered hyperfluorescent dots (microaneurysms)

surrounding the fovea with multiple tiny dots of blocked fluorescence representing retinal dot hemorrhages. (d) Fluorescein angiogram of the same eye during the late phase showing diffuse leakage (leaking microaneurysms) across the posterior pole involving the foveal avascular zone and distorting its outline

## Retinal Vein Occlusion

The clinical presentation of retinal vein occlusion (RVO) may vary according to the site of the occlusion. A branch occlusion (BRVO) typically occurs at the site of an arteriovenous crossing, while central retinal vein occlusions (CRVO) occur at the level of the lamina cribrosa (Browning 2012).

Fundus photographs reveal extensive intraretinal hemorrhage and exudation in the area drained by the occluded vein which appears tortuous and dilated. The optic nerve head may also appear elevated, hyperemic and swollen, particularly in central vein involvement. Long standing cases may

be associated with the development of optociliary collaterals, NV and the development of fibrous tissue (Hayreh et al. 1983; Murakami et al. 1983). On FA, acutely there is typically a delay in arteriovenous transit followed by staining of the walls of the affected veins. This is accompanied by capillary non-perfusion and extensive leakage distal to the site of the occlusion (Clemett 1974) (Figs. 11.8 and 11.9). In cases where the macular circulation is involved, extensive leakage of the fluorescein dye is seen in or around the fovea. In long standing ischemic cases, FA may demonstrate the development of NVD or NVE, which appear as hyperfluorescent leaking areas in the later frames (Hayreh et al. 1983).

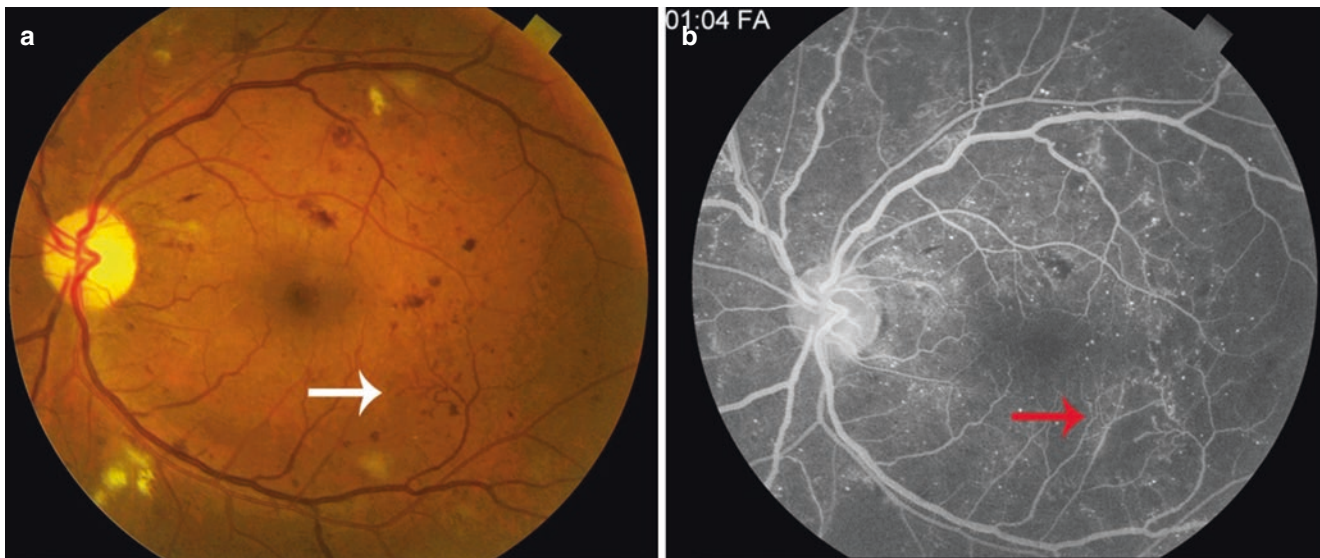


**Fig. 11.3** IRMA in very severe NPDR. (a) Fundus photo of the left eye showing multiple scattered intraretinal dot and blot hemorrhages and hard exudates across the posterior pole and outside both temporal arcades. There is a large intraretinal microvascular abnormality (IRMA) arising from the inferotemporal branch (white arrow). (b) Fluorescein

angiogram of the left eye during the late phases showing multiple scattered hyperfluorescent leaking microaneurysms with areas of blocked fluorescence (retinal hemorrhage), as well as areas of capillary non-perfusion, more obvious at the temporal and inferior periphery. The red arrow points to the hyperfluorescent IRMA, which shows no leakage

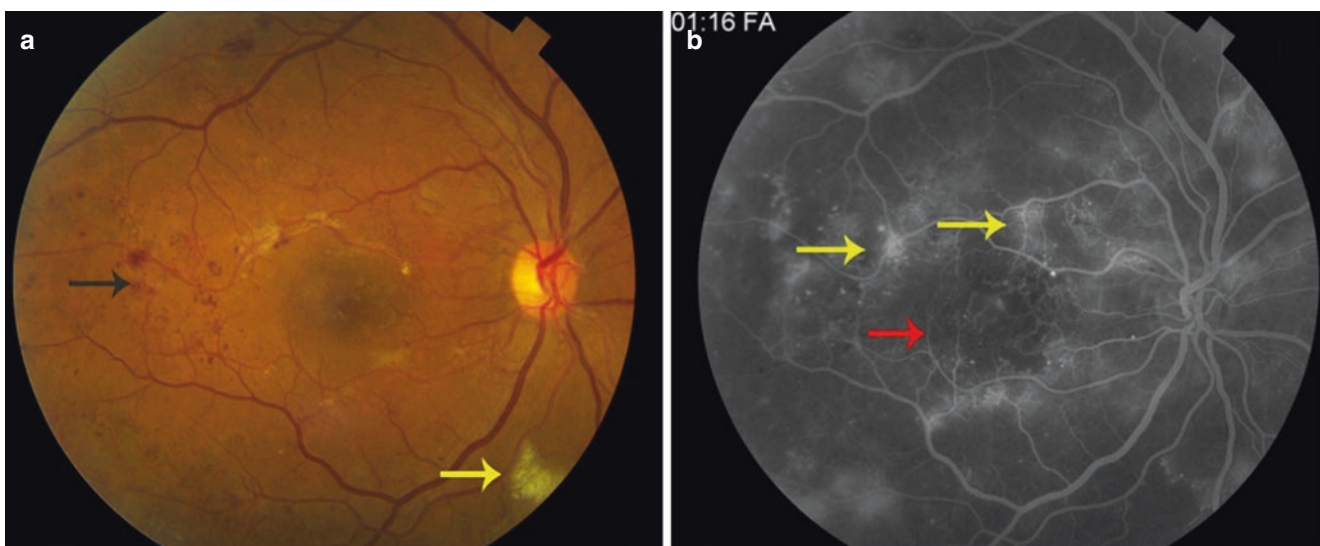


**Fig. 11.4** Enlarged FAZ in PDR. (a) Fundus photo of the right eye showing a blunt foveal reflex with multiple scattered microaneurysms and dot and blot hemorrhages across the posterior pole and along the arcades, as well as multiple areas of neovascularization (black arrow), more obvious temporal to the macula. A large cotton wool spot is seen

about 2 DD inferior to the optic disc. (b) Fluorescein angiogram of the right eye during the late phase showing multiple hyperfluorescent leaking microaneurysms and neovascularization (yellow arrows), as well as large areas of capillary non-perfusion including an enlarged foveal avascular zone (red arrow)

## Retinal Artery Occlusion

Occlusion of the retinal arterial supply may occur at different levels, including the main trunk of the central retinal artery (CRAO), one of the terminal branches of the central artery

(BRAO) or, in some cases, the cilioretinal branch of the short posterior ciliary arteries. Clinically, the diagnosis of retinal artery occlusion has commonly been based on clinical findings of retinal thickening and whitening in the area supplied by the occluded vessel. In case of CRAO, a cherry red spot



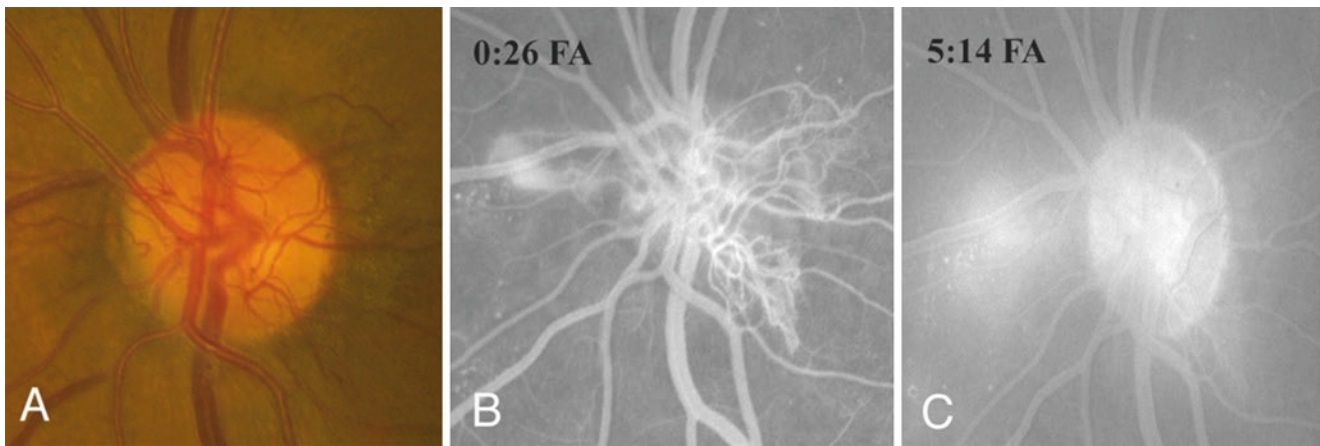


**Fig. 11.5** NVD in high-risk PDR. (a) Fundus photo of the left eye showing high risk neovascularization on the surface and surrounding the optic disc. (b) Fluorescein angiogram of the left eye during the late

venous phase showing extensive active neovascularization on the surface of the optic disc. (c) Fluorescein angiogram during the late phases showing leakage of the NVD

can be appreciated at the site of the fovea. In acute presentations, FA reveals a delay in retinal arterial filling, as well as arteriovenous transit time. FA also shows hypofluorescence of the affected area caused by thickening and swelling of the tissue and “cattle-trucking” of the blood column in the branch arteries (Beatty and Eong 2000) (Fig. 11.10).

### Sickle Cell Retinopathy

Sickle cell retinopathy is characterized by an initial non-proliferative phase characterized by vascular tortuosity, salmon patch hemorrhages between the internal limiting membrane (ILM) and the retinal surface, intraretinal hemorrhages and dark areas of RPE hyperpigmentation known as black sunbursts. Eventually, prolonged retinal ischemia and peripheral capillary non-perfusion results in the development of the proliferative phase, characterized by NV, which acquires a “sea fan” configuration, subhyaloid and/or vitreous hemorrhage as well as tractional or combined tractional-rhegmatogenous retinal detachment (Goldberg 1971).

FA remains the most widely used tool in the assessment of patients with sickle cell retinopathy to evaluate peripheral capillary non-perfusion, particularly temporally, as well as hyperfluorescent leaking NV in the earlier frames of the angiogram (Rednam et al. 1982). Owing to the peripheral nature of the retinal pathology, wide-field FA is of particular importance in these cases where some areas, particularly those close to the ora serrata, may be missed by conventional FA (Cho and Kiss 2011) (Fig. 11.11). FA may also demonstrate an enlarged FAZ. Clinically, the optic disc may exhibit small dilated capillaries that are occluded on FA (Goldbaum et al. 1978; Condon and Serjeant 1972; Moriarty et al. 1988). Later stages of sickle cell retinopathy with development of

fibroglial tissue may show staining of these membranes in the later frames of the angiogram.

## Optical Coherence Tomography in Retinal Vascular Disease

### Diabetic Macular Edema

Clinically significant macular edema (CSME) is defined as the clinical detection of any one of the following: thickening of the retina located 500  $\mu\text{m}$  or less from the center of the macula, hard exudates with thickening of the adjacent retina 500  $\mu\text{m}$  or less from the center of the macula, or a zone of retinal thickening one disc area or larger in size, located 1 disc diameter (DD) or less from the center of the macula. OCT DME is defined as thickening of the retina with or without partial loss of transparency within 1 DD from the center of the macula (Klein et al. 1995). OCT may also reveal distortion of the structural retinal anatomy caused by the accumulation of intraretinal and subretinal fluid (Hee et al. 1995) (Fig. 11.12).

OCT also provides a quantitative retinal thickness map, thus allowing easier and more thorough follow-up (Fig. 11.13). On the other hand, it is worth noting that there is no direct correlation between retinal thickness and visual acuity. Patients with higher retinal thickness may show paradoxical better visual acuity than those with lower retinal thickness, and vice versa (Network 2007) (Fig. 11.14).

Using SD-OCT, Sun et al. found a correlation between the detection of disorganization of the retinal inner layers (DRIL) in patients with DME and worsening of visual acuity (Sun et al. 2014). It may be attributed to the higher incidence of DCP affection and photoreceptor involvement associated with DRIL (Onishi et al. 2019) (Fig. 11.15).

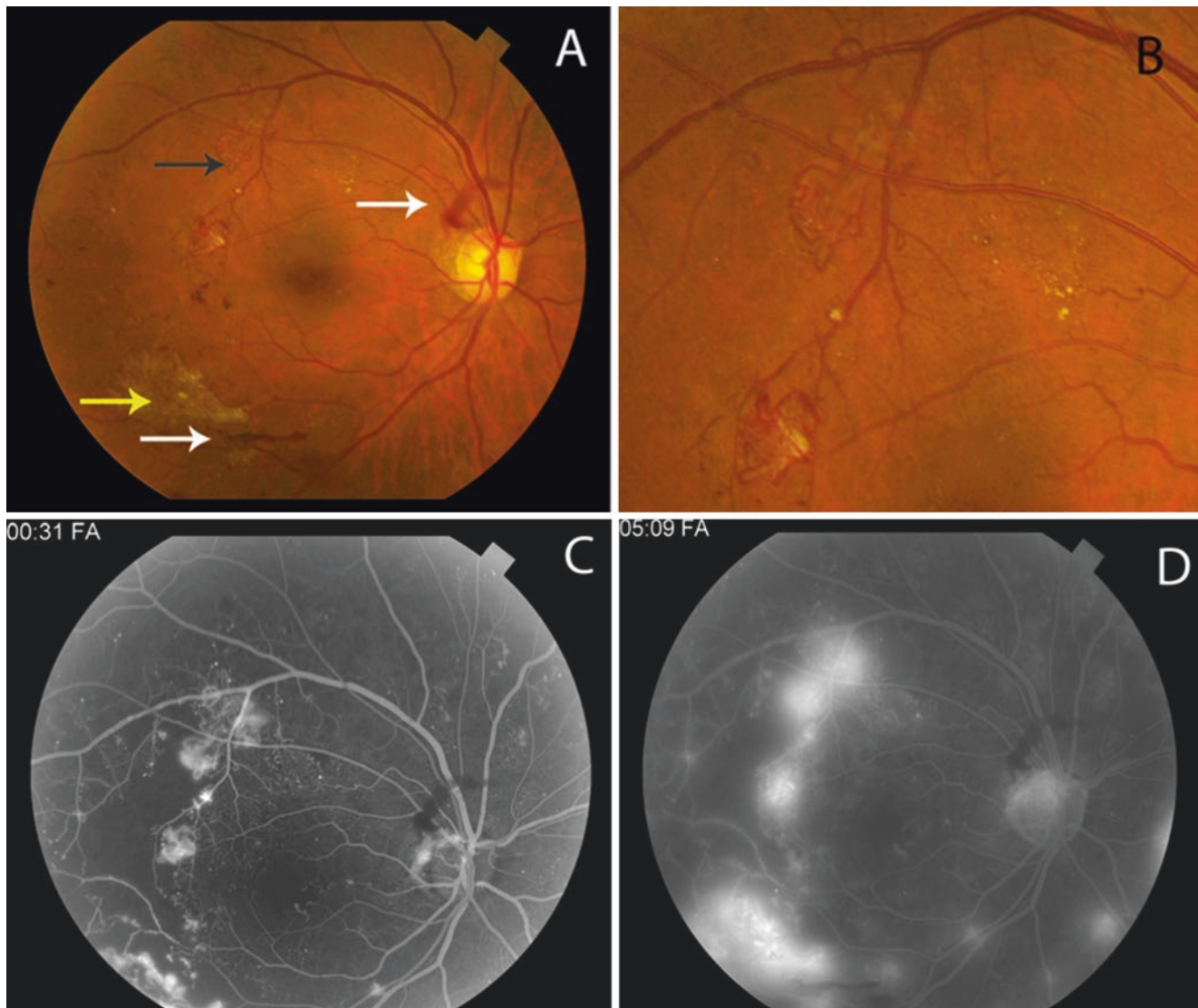


**Fig. 11.6** NVE in high-risk PDR. (a) Fundus photo of the right eye showing extensive areas of neovascularization across the superotemporal and inferotemporal arcades (black arrow) with a fibrous membrane arising inferotemporally (yellow arrow). There are multiple scattered microaneurysms, as well as two fine areas of pre-retinal hemorrhage, one superior to the optic disc and the other superior to the inferotemporal arcade (white arrows). (b) Areas of extensive neovascularization elsewhere. (c) Fluorescein angiogram of the right eye during the late

venous phase showing hyperfluorescent leakage of the temporal neovascularization and scattered microaneurysms. There is an area of blocked fluorescence caused by pre-retinal hemorrhage superior to the disc. (d) Fluorescein angiogram of the same eye during the late phases showing extensive hyperfluorescent leakage from the temporal neovascularization with the appearance of other areas of neovascularization in the inferonasal area

### Retinal Vein Occlusion

SD-OCT is a helpful tool in the assessment of the macular involvement in cases of RVO. Macular edema is typically characterized by marked thickening and/or interruption of the retinal layers accompanied by the development of hypotranslucent cystic spaces (Hee et al. 1995). Long-standing cases show higher incidences of development of epiretinal membranes, which can be readily monitored by OCT (Mitchell et al. 1997) (Fig. 11.16).

### Retinal Artery Occlusion

SD-OCT has been used in retinal artery occlusion to visualize the effect of non-perfusion on the structural integrity of the retinal layers. Increased reflectivity and thickness of the inner retina in early presentations as a result of swelling and thickening has been documented on OCT. These findings are followed by a decrease in reflectivity and thickness of the inner retina, as well as an increase in reflectivity in the outer retina and RPE/choriocapillaris layer attributed to atrophy of

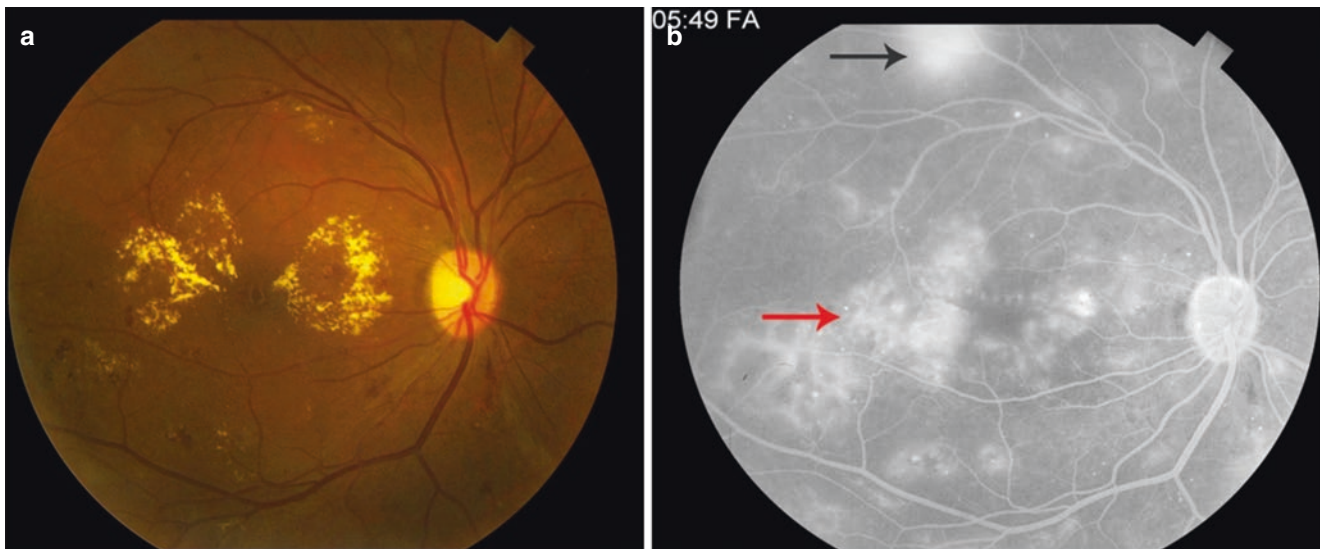


**Fig. 11.7** DME in PDR. (a) Fundus photo of the right eye showing extensive exudation surrounding the fovea forming a circinate maculopathy, as well as multiple scattered microaneurysms and dot and blot hemorrhages across the posterior pole. (b) Fluorescein angiogram of the right eye during the late phases showing multiple scattered hyper-

fluorescent microaneurysms with extensive leakage surrounding the fovea and along the inferotemporal arcade (red arrow). There is an area of hyperfluorescent leaking neovascularization along the superotemporal arcade (black arrow)

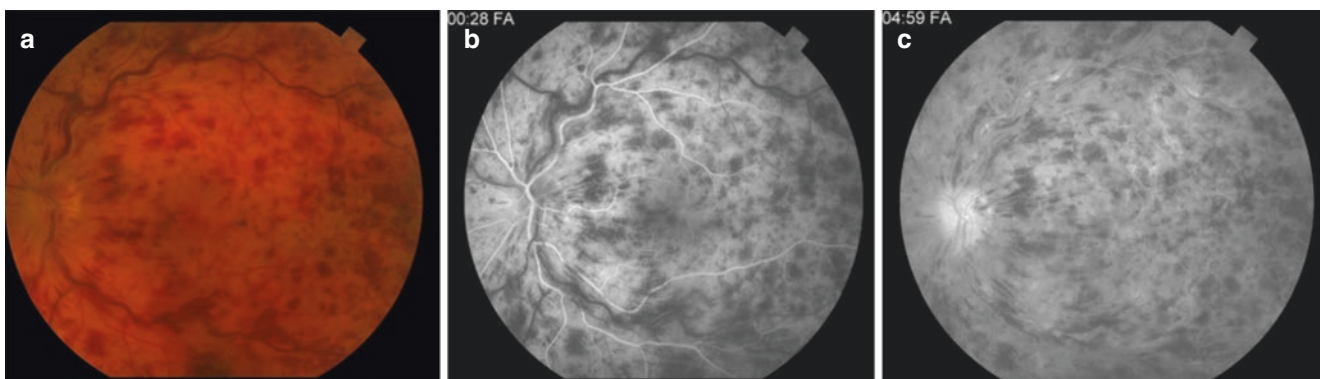


**Fig. 11.8** Central retinal vein occlusion (CRVO). (a) Fundus photo of the left eye showing markedly dilated and tortuous veins, with extensive retinal hemorrhage and cotton wool spots. The optic disc is swollen and hyperemic and the macula appears edematous. (b) Fluorescein angiogram of the left eye during the late venous phase showing marked

delay in arteriovenous transit with blocked fluorescence by extensive retinal hemorrhage and edema. (c) Fluorescein angiogram of the left eye during the late phases showing staining of the walls of the affected veins, as well as blocked fluorescence by extensive retinal hemorrhage and edema

the neurosensory retina (Ahn et al. 2015; Falkenberry et al. 2006; Yu et al. 2015).

### Acute Macular Neuroretinopathy and Paracentral Acute Middle Maculopathy

SD-OCT, as well as OCTA, have allowed better characterization of distinct manifestations of retinal ischemia named acute macular neuroretinopathy (AMN) and paracentral acute middle maculopathy (PAMM).

Clinically, AMN is characterized by the presence of intraretinal, reddish-brown, wedge-shaped lesions, commonly in the perifoveal area. A characteristic feature of these wedges is that their apices tend to point to the fovea (Bos and Deutman 1975; Bhavsar et al. 2016). They are commonly unimpressive on fundus photographs and are better appreciated on infrared imaging as parafoveal hyporeflective lesions.

FA does not add to the clinical findings and does not greatly help in the diagnosis of AMN (Priluck et al. 1978). During the acute phase of the lesion, SD-OCT shows a transient hyperreflectivity of the OPL and ONL. Within days,





**Fig. 11.9** Superotemporal branch retinal vein occlusion (BRVO). (a) Fundus photo of the left eye showing a blunt foveal reflex and extensive intraretinal hemorrhage and cotton wool spots along the superotemporal arcade extending to the macula. (b) Fluorescein angiogram of the left eye during the late venous phase showing a prolonged arteriovenous transit at the superotemporal branch of the central retinal vein.

There is noted tortuosity of the affected vein as well as blocked fluorescence secondary to the hemorrhage and edema. The leakage is seen encroaching on the foveal avascular zone. (c) Fluorescein angiogram of the left eye during the late phases showing delayed filling of the affected veins and staining of their walls with extensive exudation and hemorrhage

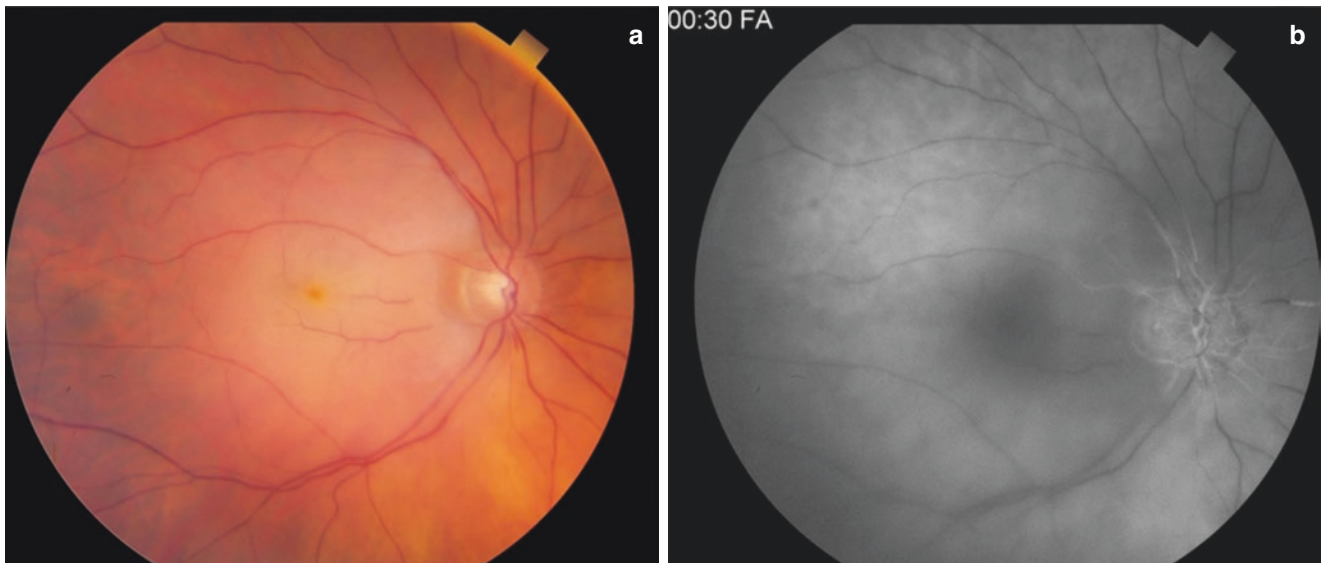


**Fig. 11.10** Central retinal artery occlusion (CRAO). (a) Fundus photo of the right eye showing marked retinal opacity at the posterior pole with the appearance of a characteristic cherry red spot at the fovea. The

vessels appear markedly attenuated. (b) Fluorescein angiogram of the right eye showing markedly delayed filling of the retinal arteries, as well as blocked fluorescence by extensive retinal edema

this hyperreflectivity begins to resolve and is followed by an interruption of the interdigitation zone (RPE/outer segment junction) and the ellipsoid zone (inner segment/outer segment junction or IS/OS), as well as thinning of the outer nuclear layer (ONL). Over time, symptoms may improve despite the persistence of some OCT findings including ONL thinning and interruption of the interdigitation zone (Fawzi et al. 2012) (Fig. 11.17).

PAMM was introduced by Sarraf et al. while documenting lesions similar to AMN but involving the middle macular

region above the outer plexiform layer (Sarraf et al. 2013). Sridhar et al. described three distinct *en face* OCT patterns in PAMM: arteriolar, fern-like, and globular (Sridhar et al. 2015). As with AMN, PAMM lesions may pass into thinning of the affected layers, primarily the inner nuclear layer (INL) (Rahimy et al. 2015) (Fig. 11.18).

As a result, SD-OCT and OCTA, in addition to near-infrared reflectance and red-free imaging, are the current imaging modalities for the detection of the subtle retinal changes associated with PAMM and AMN.





**Fig. 11.11** Proliferative sickle cell retinopathy. (a) Wide-field fundus photo (Optos) of the left eye showing markedly attenuated peripheral arteries and a black sunburst (black arrow) in the retina. There are extensive neovascularization and fibrovascular membrane formation (blue arrow) at the temporal periphery. (b) Wide-field fluorescein angiogram of the left eye during the early venous phase showing an area

of blocked fluorescence nasally (black sunburst) (white arrows) as well as extensive peripheral non-perfusion (red arrow). (c) Fluorescein angiogram of the left eye during the late phases showing additional hyperfluorescent leaking neovascularization (yellow arrows) at the temporal periphery as well as inferonasally

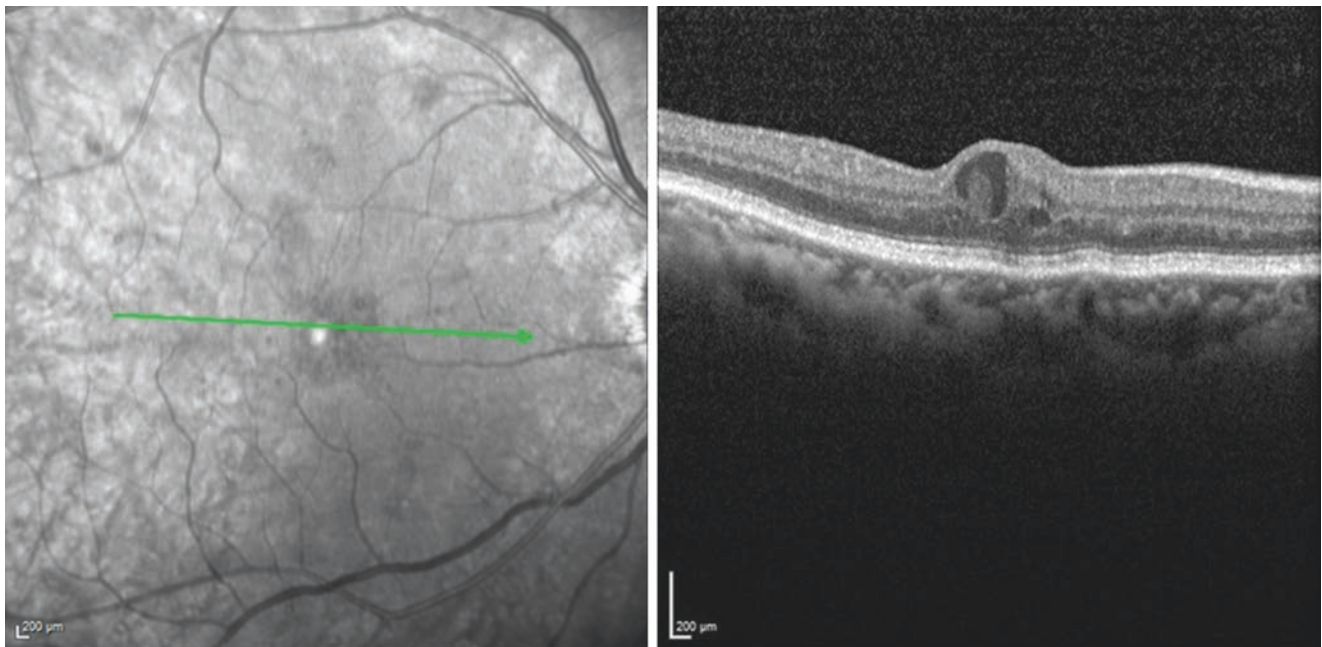


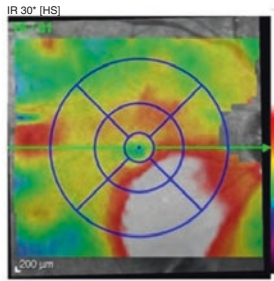
**Fig. 11.12** Diabetic macular edema (DME). Spectral domain optical coherence tomography (SD-OCT) showing retinal thickening and formation of intraretinal cystic spaces involving the fovea

**Thickness Map Change Report, Recent Follow-up**  
SPECTRALIS® Tracking Laser Tomography

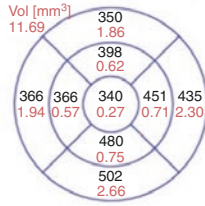


Patient: \_\_\_\_\_ DOB: \_\_\_\_\_ Sex: \_\_\_\_\_  
 Patient ID: \_\_\_\_\_ Comment: --- OD  
 Diagnosis: ---

Reference Mar/27/2017

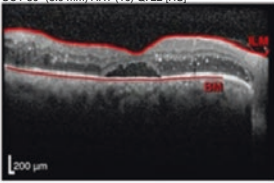


Average Thickness [µm]

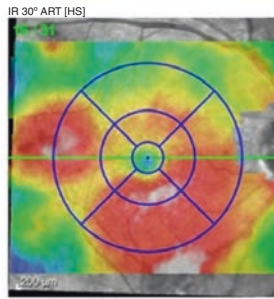


Center: 284 µm  
 Central Min: 275 µm  
 Central Max: 414 µm  
 Circle Diameters:  
 1, 3, 6 mm ETDRS

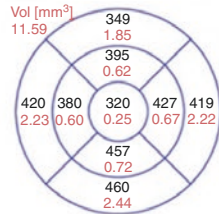
OCT 30° (8.9 mm) ART (16) Q: 22 [HS]



Follow-Up #2 Jun/26/2017

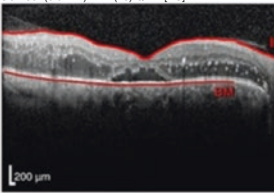


Average Thickness [µm]

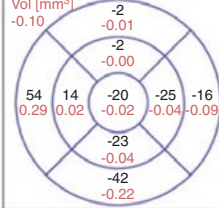


Center: 266 µm  
 Central Min: 255 µm  
 Central Max: 381 µm  
 Circle Diameters:  
 1, 3, 6 mm ETDRS

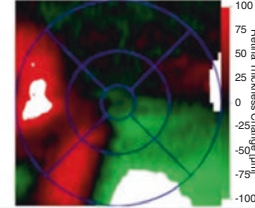
OCT 30° (8.9 mm) ART (15) Q: 22 [HS]



Average Change [µm]



Thickness Change [µm]



Software Version: 6.3.4

www.HeidelbergEngineering.com

Thickness Map Change Report, Recent Follow-Up

**Fig. 11.13** OCT retinal thickness map. Optical coherence tomography retinal thickness map of the right eye of a patient with center involving diabetic macular edema. A 3-month follow-up scan (below) reveals a decrease in the central foveal thickness, as well as in overall volume. Blue arrows show B scans from both visits. Black arrows show color

coded maps of retinal elevation. Red arrows indicate retinal thickness in the nine ETDRS sectors. Yellow arrow shows the difference in retinal thickness between both visits using ETDRS sectors and a color coded map



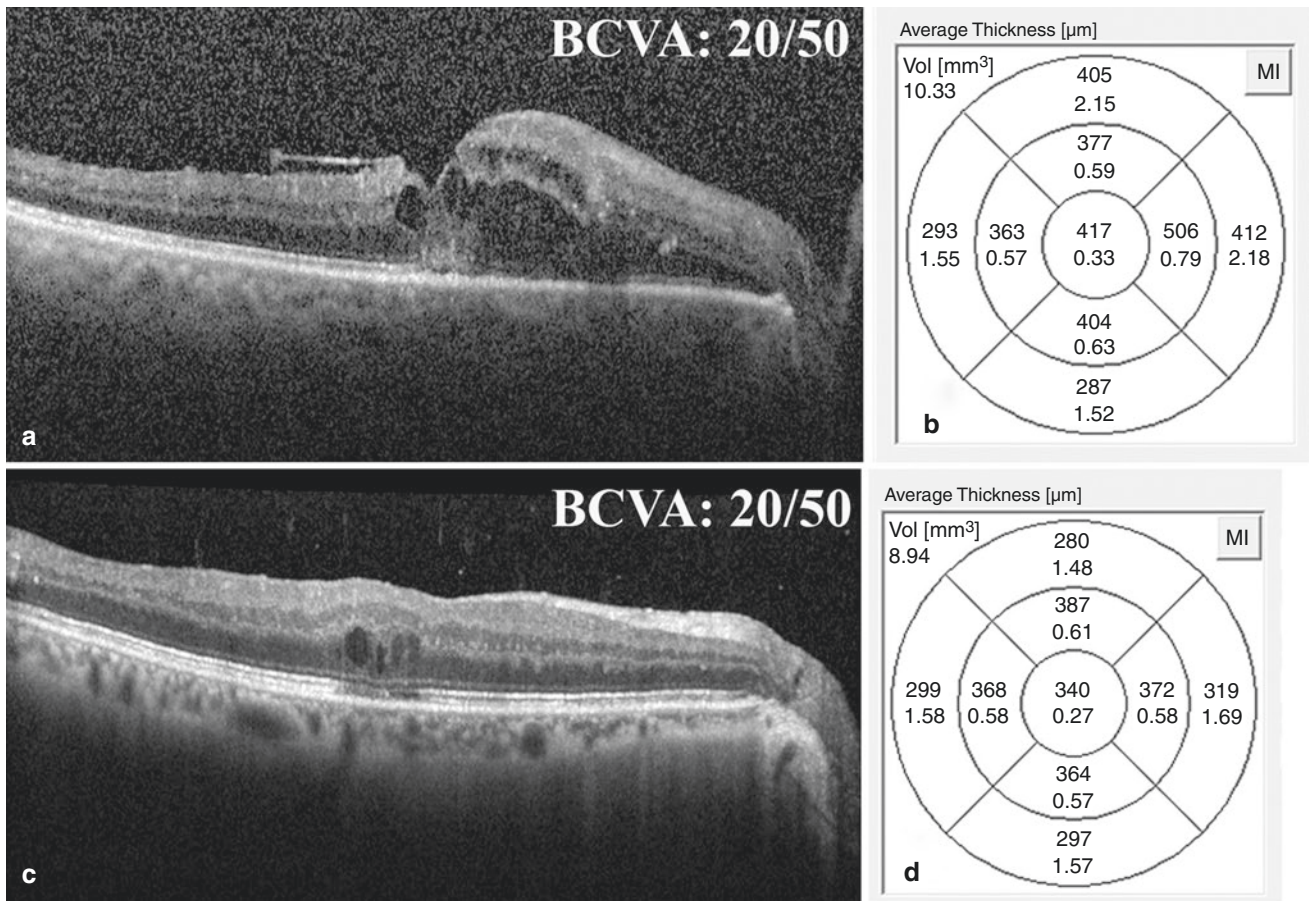


**Fig. 11.14** BCVA does not correlate with retinal thickness. (a and c) SD-OCT of the right eye of two patients with DME and NPDR. (b) Retinal thickness map of patient (a). The central foveal thickness (CFT) is 417  $\mu\text{m}$  and the retinal volume is 10.33  $\text{mm}^3$ . (d) Retinal thickness

map of patient (c). The CFT is 340  $\mu\text{m}$  while the retinal volume is 8.94  $\text{mm}^3$ . Both patients had a BCVA of 20/50 despite the difference in retinal thickness

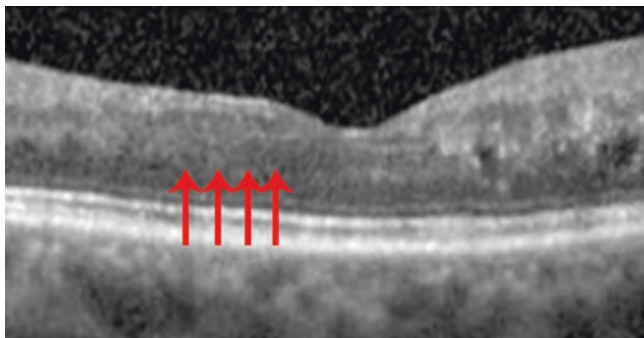


**Fig. 11.15** Disorganized retinal inner layers (DRIL). Spectral domain optical coherence tomography (SD-OCT) of the right eye. There is predominant retinal thinning temporally, with clear disorganization of the inner retinal layers (DRIL) (red arrows)

### Sickle Cell Retinopathy

SD-OCT is helpful in demonstrating the consequences of sickle ischemic maculopathy, even in cases that are undetectable on FA. Murthy et al. found atrophy of the inner retinal layers of patients with sickle cell retinopathy (Murthy et al. 2011). This finding was also corroborated by Witkin et al. and was attributed to the occurrence of a macular infarction as a result of an ischemic vaso-occlusive episode (Witkin et al. 2006) (Fig. 11.19). Chen et al. demonstrated preferential ischemia of the DCP in sickle cell retinopathy, which resulted in selective atrophy of the middle layers of the macula on SD-OCT (Chen et al. 2015).

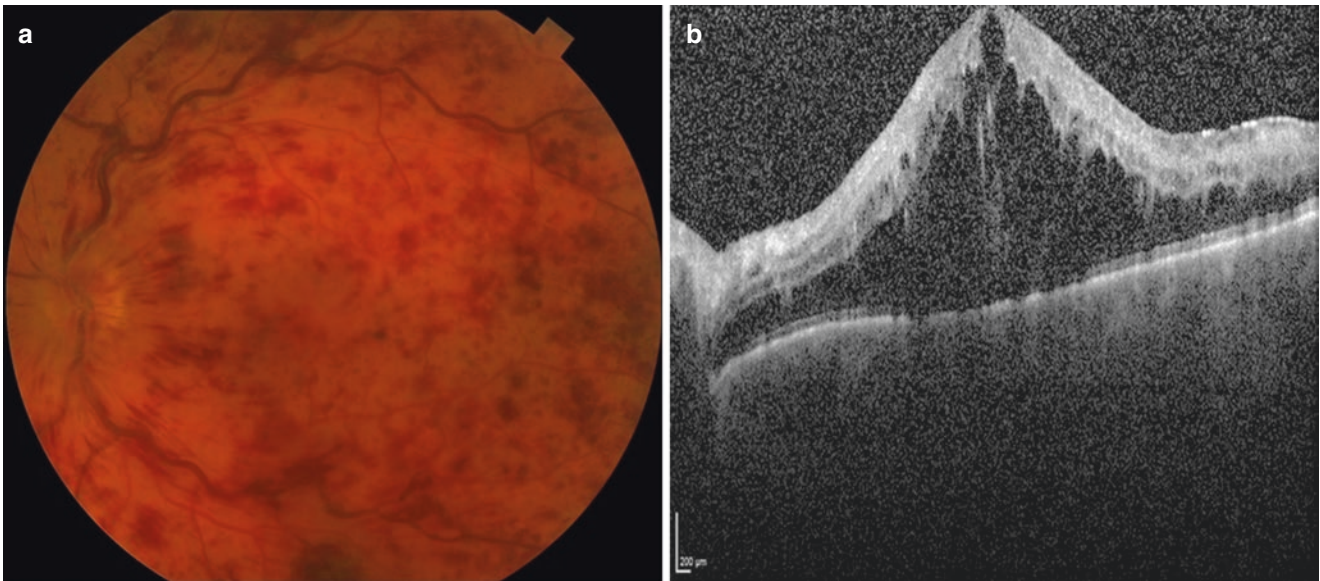


**Fig. 11.16** OCT of CME in CRVO. (a) Fundus photo of the left eye showing markedly dilated and tortuous veins, with extensive retinal hemorrhage and cotton wool spots. The optic disc is swollen and hyperemic and the macula appears edematous. (b) Spectral domain optical

coherence tomography (SD-OCT) showing cystoid macular edema with multiple intraretinal cysts extending from the outer plexiform layer

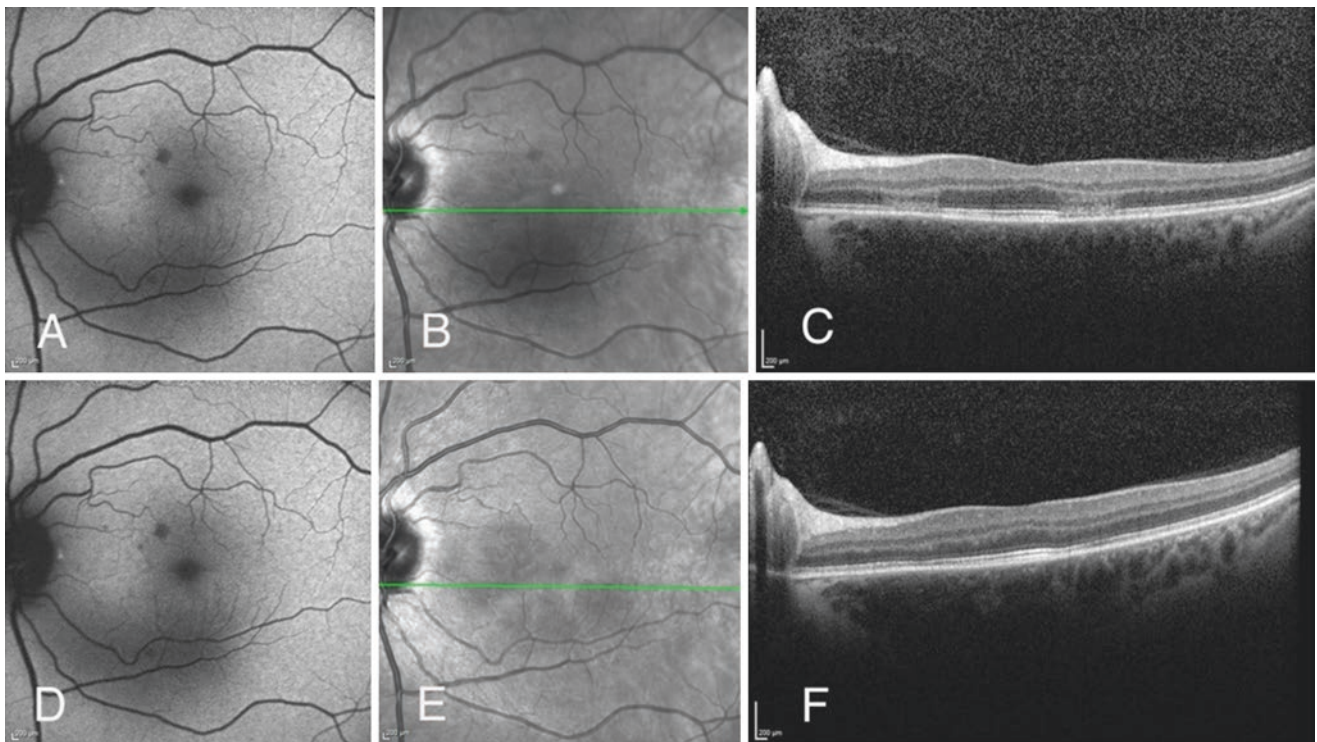


**Fig. 11.17** Acute macular neuroretinopathy (AMN). (a and b) Fundus autofluorescence and infrared images of the left eye with AMN not clearly showing the hyporeflective lesions during the early phase. (c) Spectral domain optical coherence tomography (SD-OCT) showing hyperreflectivity of the outer nuclear layer. (d) FAF 1 month later with

no significant change. (e) IR 1 month later showing a more clear image of the hyporeflective perifoveal lesions. (f) SD-OCT 1 month later showing marked improvement of the outer retinal layers with slight residual affection of the interdigitation zone (OS/RPE junction)



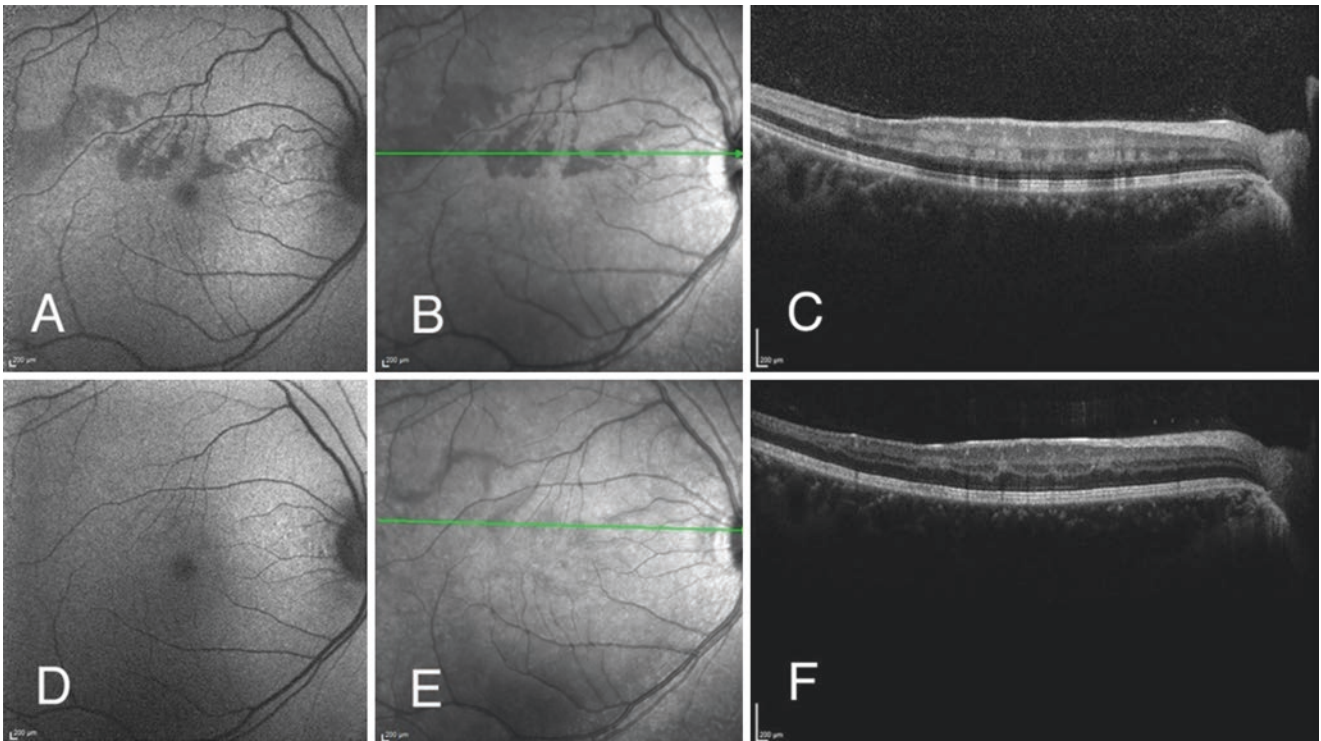


**Fig. 11.18** Paracentral acute middle maculopathy (PAMM) in the setting of a small retinal branch superior vein occlusion. (a) Fundus autofluorescence photo of the right eye with PAMM showing areas of patchy hypoautofluorescence superior and temporal to the fovea corresponding to the swollen non-perfused area. (b) Infrared photograph of the right eye showing the hyporeflective perifoveal lesions. (c) Spectral

domain optical coherence tomography (SD-OCT) showing multiple hyperreflective bands affecting the outer plexiform, inner nuclear, and inner plexiform layers. (d and e) FAF and IR 2 months later showing marked resolution of the perifoveal lesions. (f) SD-OCT 2 months later showing atrophy of the inner nuclear layer

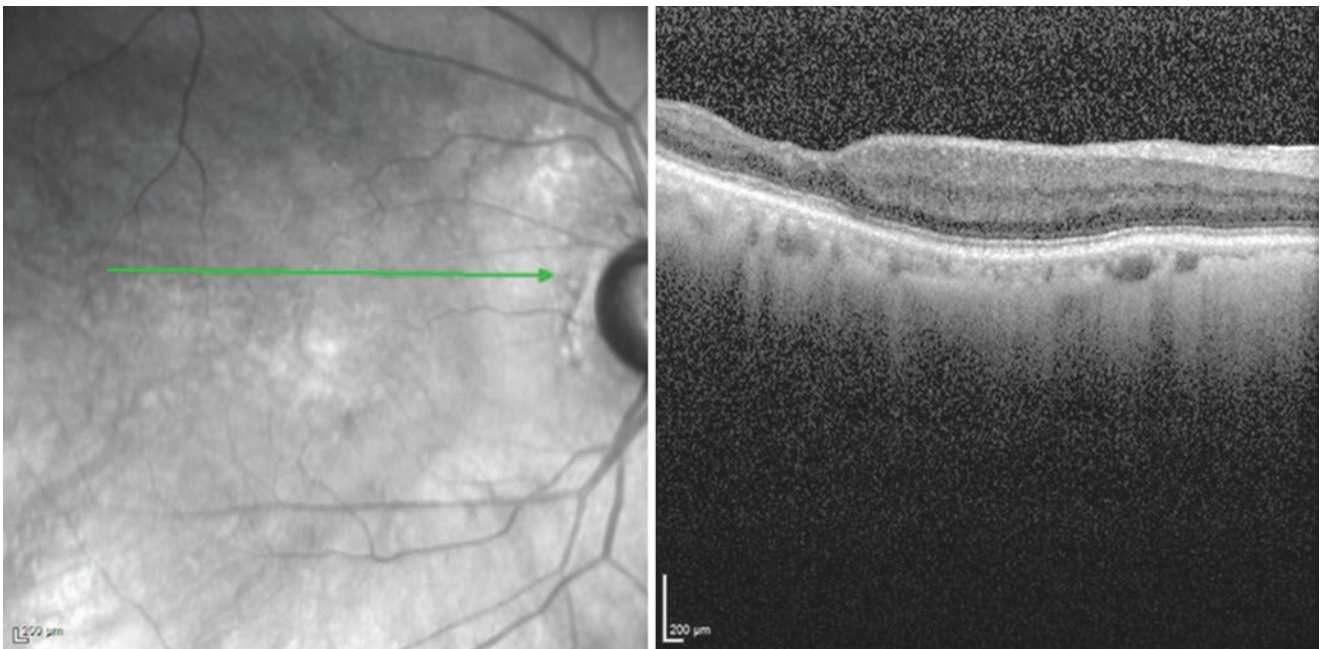


**Fig. 11.19** OCT in sickle cell retinopathy. IR photo and SD-OCT of the right eye showing areas of marked inner retinal thinning superotemporal to the fovea in a patient with sickle cell retinopathy



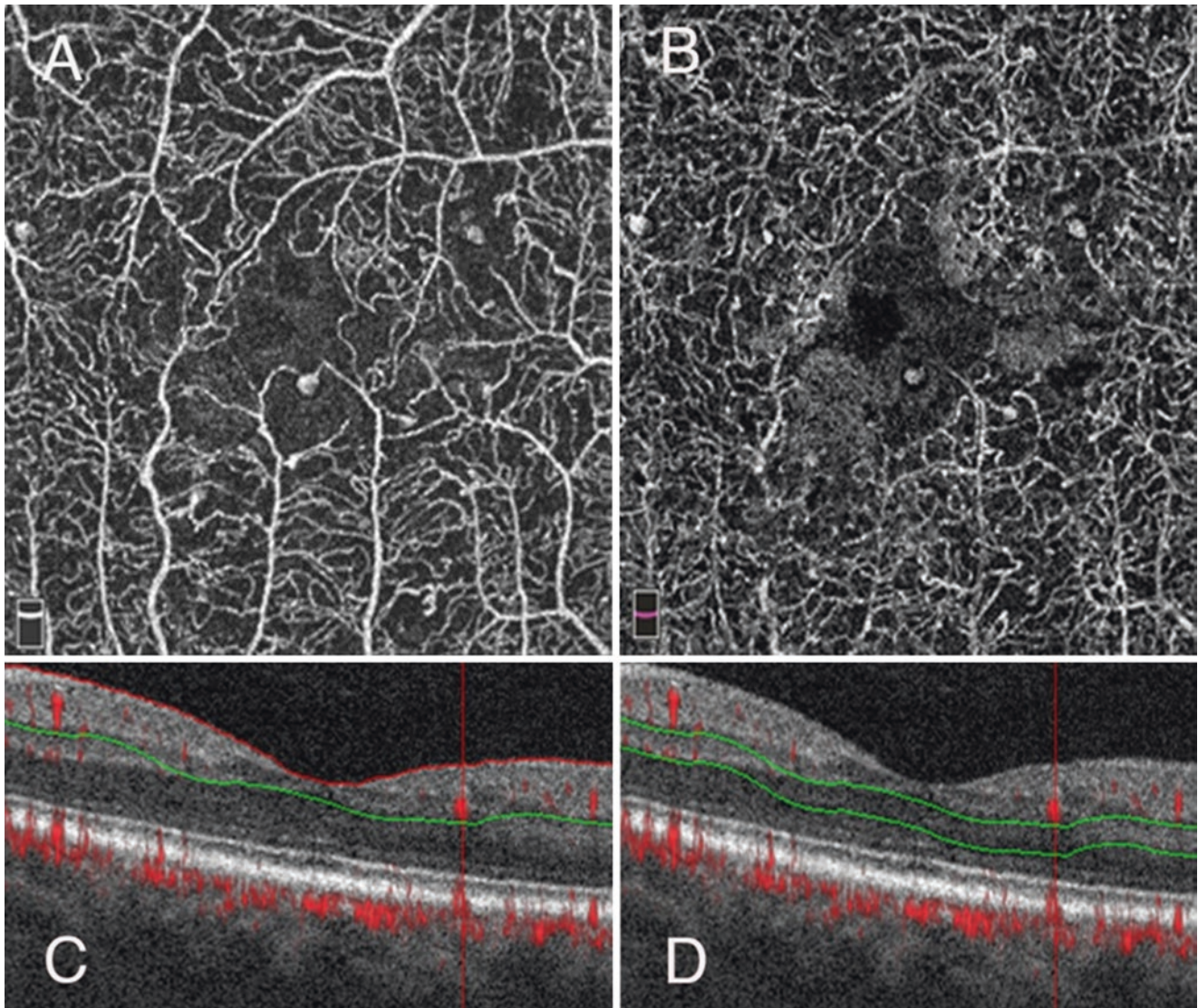


**Fig. 11.20** OCTA of microaneurysms. A  $3 \times 3$  mm OCT angiogram segmented at the superficial (a) and deep (b) retinal capillary plexus. Microaneurysms appear as multiple dilated sacculi arising at the ends

of capillary branches. B-scan OCTA segmented at the superficial (c) and deep (d) plexuses. Notice the microaneurysm in (c) at the junction between the red and green lines

## Optical Coherence Tomography Angiography in Retinal Vascular Disease

### Diabetic Retinopathy

In DR, OCTA shows microaneurysms as focally dilated capillaries contiguous with neighboring capillaries (Fig. 11.20). The visualization of microaneurysms can be enhanced by separating the vascular layers into SCP, MCP, and DCP, which enabled Choi et al. to determine that microaneurysms tend to be more detectable in the intermediate plexus (Huang et al. 2017; Choi et al. 2017).

OCTA is beneficial in cases where IRMAs may be confused with areas of NVE by assessing the level of these vessels with respect to the internal limiting membrane (ILM). *En Face* images of the SCP will identify IRMAs whereas images above the ILM will detect NV extending into the vitreous (de Carlo et al. 2016) (Fig. 11.21).

The advantage of OCTA over FA is that it consistently provides images that present a more accurate description of capillary non-perfusion, NV, and size of the FAZ because the image is not occluded by dye leakage (Al-Sheikh et al. 2016; Samara et al. 2017; Couturier et al. 2015). Images obtained by OCTA have the added advantage of separating



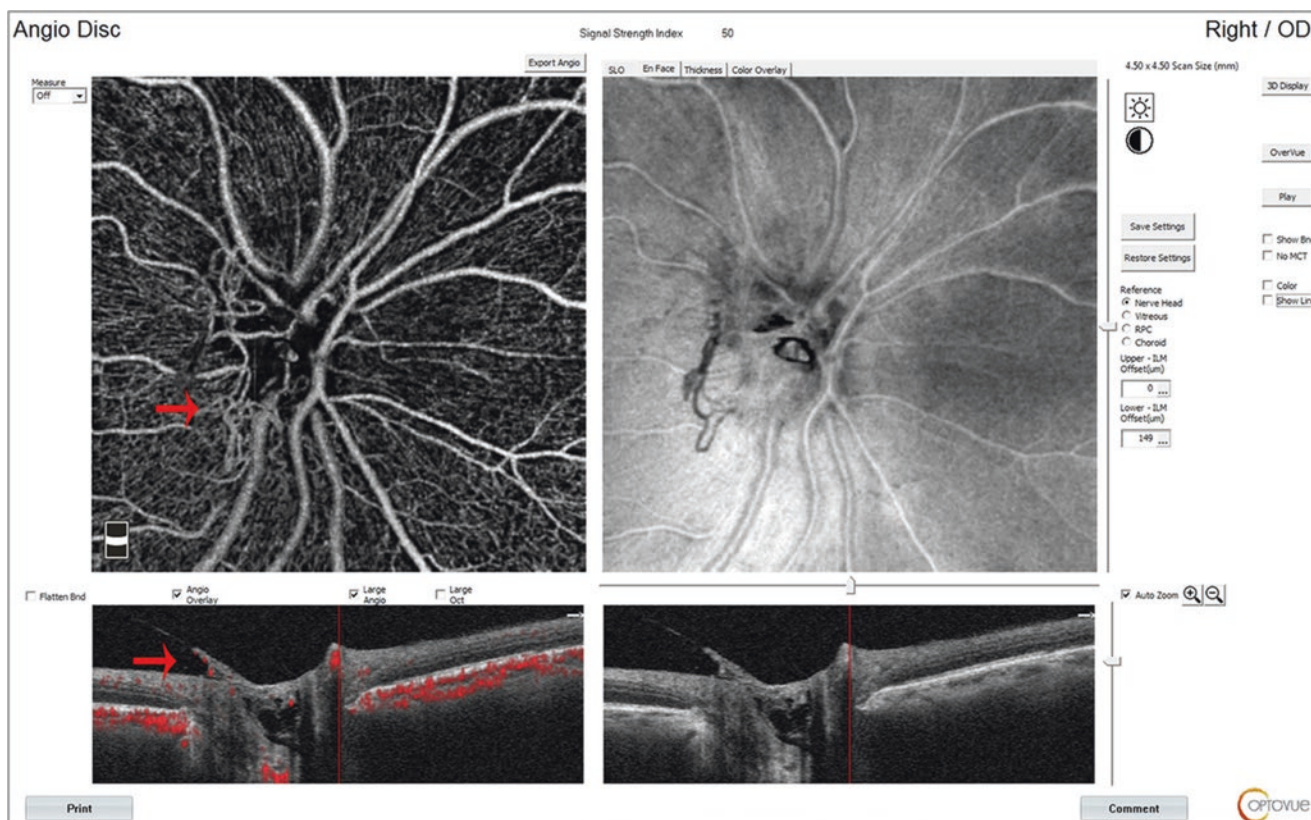


**Fig. 11.21** OCTA of NVD.  $4.5 \times 4.5$  mm optical coherence tomography angiography (OCTA) scan segmented to visualize the vessels of the optic nerve head showing areas of neovascularization (red arrow) arising

along the nasal border of the optic nerve, with a B scan showing neovascularization extending to the vitreous

retinal vessels into distinct layers (up to 3 in the macular area), which allows a more thorough examination of the effect of non-perfusion in each layer.

OCTA has also been helpful in understanding the contribution of the DCP to the oxygen requirements of the photoreceptor and outer retinal layers. Scarinci et al. found areas of capillary disruption in the DCP that corresponded to photoreceptor disruption on the SD-OCT, suggesting the importance of the DCP for the metabolic demand of the photoreceptors (Scarinci et al. 2016).

## Retinal Vein Occlusion

Compared to FA, OCTA has the additional advantage of demonstrating the SCP and DCP with less interference of the retinal hemorrhage and dye leakage (Rispoli et al. 2015) (Fig. 11.22). Coscas et al. determined that, in RVO, the grayish non-perfused areas and the disrupted and dilated capillary network were more frequent in the DCP than the SCP

(Coscas et al. 2016). This provides evidence that retinal vein occlusion affects the deeper plexus more severely than it affects the superficial plexus.

OCTA is also effective in the evaluation of the ischemic non-perfused areas in the retina, especially those involving the macula (Cardoso et al. 2016). This can be a very important prognostic tool in the prediction of visual recovery in some cases. Both Suzuki et al. and Chung et al. found that OCTA was superior in detecting eyes with capillary non-perfusion when compared to FA because it provided higher-resolution images (Suzuki et al. 2016; Chung et al. 2017). On the other hand, OCTA cannot detect non-perfused areas in the peripheral retina which are readily picked up by wide-field FA due to limited field of view (Suzuki et al. 2016).

Iida et al. used OCTA to challenge previously reported patterns of arteriovenous crossing in cases of BRVO by documenting a higher number of cases with venous overcrossing than FA was able to detect. They also noticed more venous narrowing and macular non-perfusion in these cases (Iida et al. 2017).

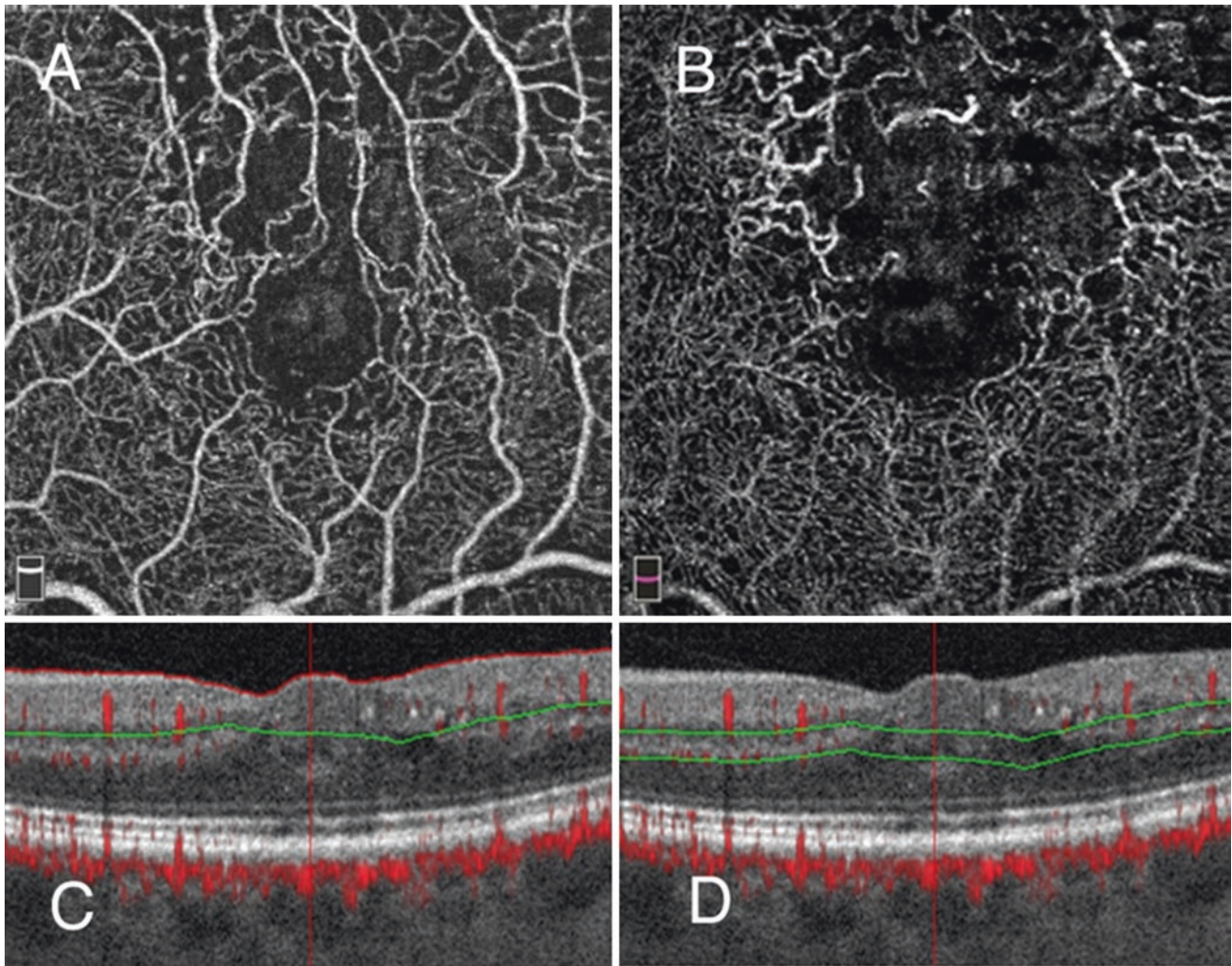


**Fig. 11.22** OCTA of BRVO. 3 × 3 mm optical coherence tomography angiography (OCTA) centered around the fovea and segmented to show the superficial (a) and deep (b) retinal capillary plexuses. The vessels superior to the foveal avascular zone are enlarged and irregular and

appear separated by the accumulating retinal fluid. These changes are more evident in the deeper plexus. (c and d) B scan OCTA segmented at the superficial (c) and deep (d) plexuses showing spongy retinal edema with a few intraretinal cystic spaces

### Retinal Artery Occlusion

Bonini Filho et al. (2015) described areas of non-perfusion in both SCP and DCP using OCTA. de Castro-Abeger et al. determined that OCTA was superior to FA in detecting perfusion defects in the SCP. This is due to the ability of OCTA to better visualize the vasculature in areas with retinal swelling (de Castro-Abeger et al. 2015).

### Acute Macular Neuroretinopathy and Paracentral Acute Middle Maculopathy

Patients with AMN and PAMM present with hyperreflective retinal layers, thought to represent the effect of a retinal vascular insult. This hypothesis can be validated using OCTA by

demonstrating areas of DCP defects (Pecen et al. 2015) (Fig. 11.23).

### Sickle Cell Retinopathy

OCTA provides high-resolution images of the ischemic changes affecting the macula, which can shed light on the prognosis of visual affection and recovery in patients with sickle cell retinopathy. Minvielle et al. identified rarefied and dilated capillaries and enlargement of the FAZ in both SCP and DCP in all their patients with sickle cell retinopathy (Minvielle et al. 2016). They also noted capillary non-perfusion in the SCP of 72.2%, and in the DCP of 27.8% of their patients. Most capillary abnormalities were located in the temporal juxtafoveal region and might extend to the superior and inferior juxtafoveal regions.



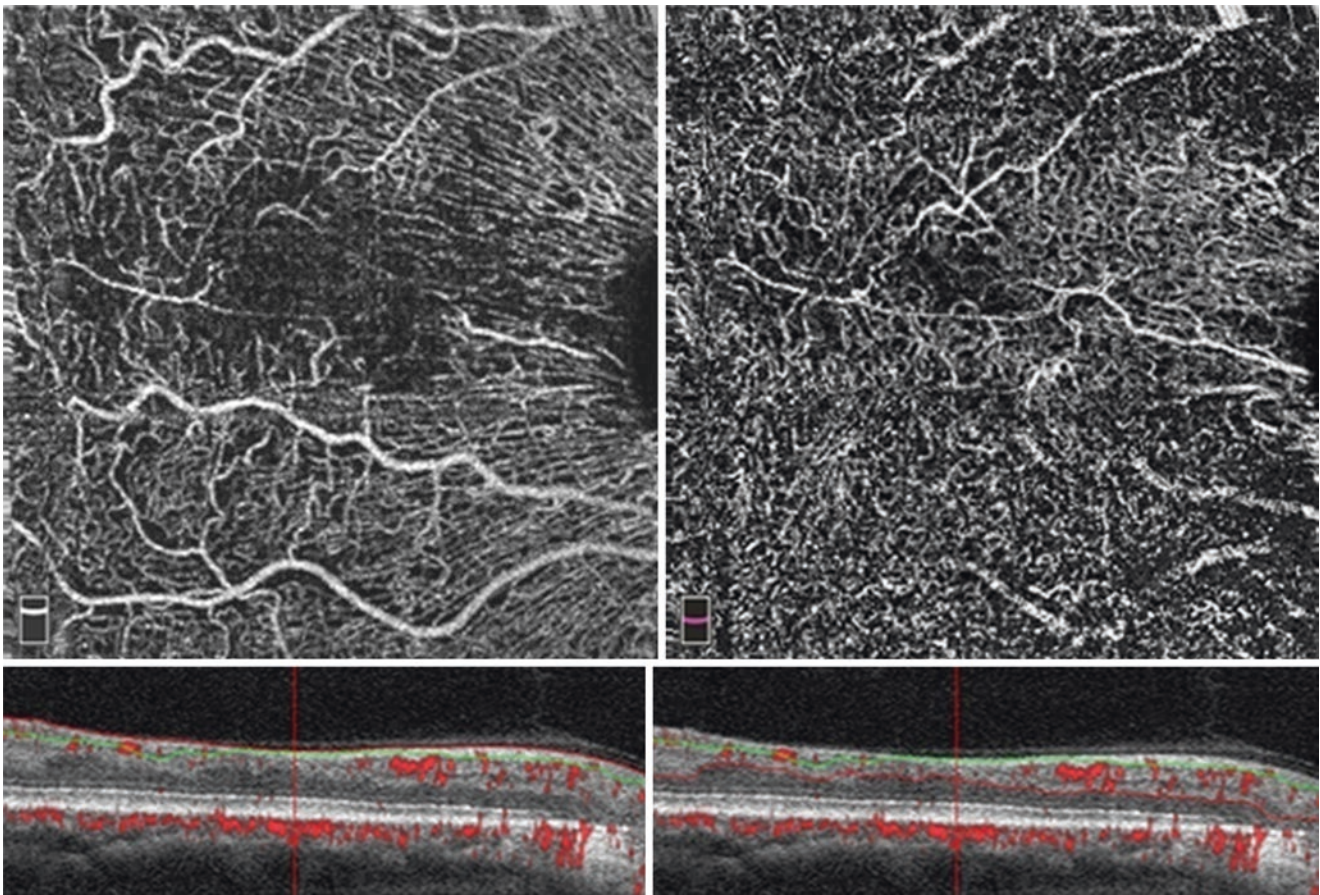


**Fig. 11.23** OCTA of PAMM. 3 × 3 mm *en face* OCTA centered around a PAMM lesion temporal to the optic disc and segmented to show the superficial (left) and deep (right) retinal capillary plexuses. They show

areas of capillary non-perfusion (as evident by both *en face* and flow projection) corresponding to the atrophic areas of the inner nuclear layer

In sickle cell retinopathy, OCTA can also be used to visualize abnormal NV developing at or around the optic disc as well as surrounding the macula. However, due to its limited access to the retinal periphery where most of the pathology is, wide-field FA remains superior to OCTA in the assessment of sickle cell retinopathy, especially in the proliferative stages.

## References

- Ahn SJ, Woo SJ, Park KH, Jung C, Hong J-H, Han M-K. Retinal and choroidal changes and visual outcome in central retinal artery occlusion: an optical coherence tomography study. *Am J Ophthalmol.* 2015;159(4):667–76.e661.
- Akram MU, Khalid S, Khan SA. Identification and classification of microaneurysms for early detection of diabetic retinopathy. *Pattern Recogn.* 2013;46(1):107–16.
- Al-Sheikh M, Akil H, Pfau M, Sadda SR. Swept-source OCT angiography imaging of the foveal avascular zone and macular capillary network density in diabetic retinopathy OCT-angiography in diabetic retinopathy. *Invest Ophthalmol Vis Sci.* 2016;57(8):3907–13.
- Arend O, Wolf S, Harris A, Reim M. The relationship of macular microcirculation to visual acuity in diabetic patients. *Arch Ophthalmol.* 1995;113(5):610–4.
- Beatty S, Eong KA. Acute occlusion of the retinal arteries: current concepts and recent advances in diagnosis and management. *Emerg Med J.* 2000;17(5):324–9.
- Bhavsar KV, Lin S, Rahimy E, Joseph A, Freund KB, Sarraf D, Cunningham ET. Acute macular neuroretinopathy: a comprehensive review of the literature. *Surv Ophthalmol.* 2016;61(5):538–65.
- Bonini Filho MA, Adhi M, Talisa E, Ferrara D, Baumal CR, Witkin AJ, Reichel E, Kuehlewein L, Sadda SR, Sarraf D. Optical coherence tomography angiography in retinal artery occlusion. *Retina.* 2015;35(11):2339–46.
- Bos PJ, Deutman AF. Acute macular neuroretinopathy. *Am J Ophthalmol.* 1975;80(4):573–84.
- Bresnick GH, Condit R, Syrjala S, Palta M, Groo A, Korth K. Abnormalities of the foveal avascular zone in diabetic retinopathy. *Arch Ophthalmol.* 1984;102(9):1286–93.
- Browning DJ. Anatomy and pathologic anatomy of retinal vein occlusions. In: Browning DJ, editor. *Retinal vein occlusions: evidence-based management.* New York: Springer; 2012. p. 1–31. [https://doi.org/10.1007/978-1-4614-3439-9\\_1](https://doi.org/10.1007/978-1-4614-3439-9_1).
- Cardoso JN, Keane PA, Sim DA, Bradley P, Agrawal R, Addison PK, Egan C, Tufail A. Systematic evaluation of optical coherence tomography angiography in retinal vein occlusion. *Am J Ophthalmol.* 2016;163:93–107.e6.

- Chen X, Rahimy E, Sergott RC, Nunes RP, Souza EC, Choudhry N, Cutler NE, Houston SK, Munk MR, Fawzi AA. Spectrum of retinal vascular diseases associated with paracentral acute middle maculopathy. *Am J Ophthalmol*. 2015;160(1):26–34.e21.
- Chew EY, Klein ML, Ferris FL, Remaley NA, Murphy RP, Chantry K, Hoogwerf BJ, Miller D. Association of elevated serum lipid levels with retinal hard exudate in diabetic retinopathy: early treatment diabetic retinopathy study (ETDRS) report 22. *Arch Ophthalmol*. 1996;114(9):1079–84.
- Cho M, Kiss S. Detection and monitoring of sickle cell retinopathy using ultra wide-field color photography and fluorescein angiography. *Retina*. 2011;31(4):738–47.
- Choi W, Waheed NK, Moulton EM, Adhi M, Lee B, De Carlo T, Jayaraman V, Bauman CR, Duker JS, Fujimoto JG. Ultrahigh speed swept source optical coherence tomography angiography of retinal and choriocapillaris alterations in diabetic patients with and without retinopathy. *Retina*. 2017;37(1):11–21.
- Chung CY, Tang HHY, Li SH, Li KKW. Differential microvascular assessment of retinal vein occlusion with coherence tomography angiography and fluorescein angiography: a blinded comparative study. *Int Ophthalmol*. 2017;38:1–10.
- Clemett RS. Retinal branch vein occlusion. Changes at the site of obstruction. *Br J Ophthalmol*. 1974;58(5):548.
- Condon PI, Serjeant GR. Ocular findings in homozygous sickle cell anemia in Jamaica. *Am J Ophthalmol*. 1972;73(4):533–43.
- Conrath J, Giorgi R, Raccach D, Ridings B. Foveal avascular zone in diabetic retinopathy: quantitative vs qualitative assessment. *Eye*. 2005;19(3):322.
- Coscas F, Glacet-Bernard A, Miere A, Caillaux V, Uzzan J, Lupidi M, Coscas G, Souied EH. Optical coherence tomography angiography in retinal vein occlusion: evaluation of superficial and deep capillary plexa. *Am J Ophthalmol*. 2016;161:160–171.e62.
- Couturier A, Mané V, Bonnin S, Erginay A, Massin P, Gaudric A, Tadayoni R. Capillary plexus anomalies in diabetic retinopathy on optical coherence tomography angiography. *Retina*. 2015;35(11):2384–91.
- Davis MD, Norton EW, Myers FL. The Airlie classification of diabetic retinopathy. In: *Symposium on the treatment of diabetic retinopathy*. Airlie House, Warrenton; 1968. p. 7–37.
- de Carlo TE, Bonini Filho MA, Bauman CR, Reichel E, Rogers A, Witkin AJ, Duker JS, Waheed NK. Evaluation of preretinal neovascularization in proliferative diabetic retinopathy using optical coherence tomography angiography. *Ophthalmic Surg Lasers Imaging Retina*. 2016;47(2):115–9.
- de Castro-Abeger AH, de Carlo TE, Duker JS, Bauman CR. Optical coherence tomography angiography compared to fluorescein angiography in branch retinal artery occlusion. *Ophthalmic Surg Lasers Imaging Retina*. 2015;46(10):1052–4.
- de Venecia G, Davis M, Engerman R. Clinicopathologic correlations in diabetic retinopathy: I. Histology and fluorescein angiography of microaneurysms. *Arch Ophthalmol*. 1976;94(10):1766–73.
- Falkenberry SM, Ip MS, Blodi BA, Gunther JB. Optical coherence tomography findings in central retinal artery occlusion. *Ophthalmic Surg Lasers Imaging Retina*. 2006;37(6):502–5.
- Fawzi AA, Pappuru RR, Sarraf D, Le PP, McCannel CA, Sobrin L, Goldstein DA, Honowitz S, Walsh AC, Sadda SR. Acute macular neuroretinopathy: long-term insights revealed by multimodal imaging. *Retina*. 2012;32(8):1500–13.
- Ferris FL, Patz A. Macular edema. A complication of diabetic retinopathy. *Surv Ophthalmol*. 1984;28:452–61.
- Goldbaum MH, Jampol LM, Goldberg MF. The disc sign in sickling hemoglobinopathies. *Arch Ophthalmol*. 1978;96(9):1597–600.
- Goldberg MF. Classification and pathogenesis of proliferative sickle retinopathy. *Am J Ophthalmol*. 1971;71(3):649–65.
- Grant MB, Luty GA. *Retinal and choroidal vasculature*. Retinal oxygenation (Retina 5th edn). Elsevier; 2012.
- Hayreh SS, Rojas P, Podhajsky P, Montague P, Woolson RF. Ocular neovascularization with retinal vascular occlusion-III: incidence of ocular neovascularization with retinal vein occlusion. *Ophthalmology*. 1983;90(5):488–506.
- Hee MR, Puliafito CA, Wong C, Duker JS, Reichel E, Rutledge B, Schuman JS, Swanson EA, Fujimoto JG. Quantitative assessment of macular edema with optical coherence tomography. *Arch Ophthalmol*. 1995;113(8):1019–29.
- Huang D, Lumbroso B, Jia Y, Waheed NK. *Optical coherence tomography angiography of the eye*. SLACK Incorporated; 2017.
- Iida Y, Muraoka Y, Ooto S, Suzuma K, Murakami T, Iida-Miwa Y, Ghashut R, Tsujikawa A. Morphologic and functional retinal vessel changes in branch retinal vein occlusion: an optical coherence tomography angiography study. *Am J Ophthalmol*. 2017;182:168.
- Jakobiec FA. *Ocular anatomy, embryology, and teratology*. Philadelphia: Harpercollins; 1982.
- Justice J, Lehmann RP. Cilioretinal arteries: a study based on review of stereo fundus photographs and fluorescein angiographic findings. *Arch Ophthalmol*. 1976;94(8):1355–8.
- Klein R, Klein BE, Moss SE, Cruickshanks KJ. The Wisconsin epidemiologic study of diabetic retinopathy XV: the long-term incidence of macular edema. *Ophthalmology*. 1995;102(1):7–16.
- Max Snodderly D, Weinhaus RS. Retinal vasculature of the fovea of the squirrel monkey, *Saimiri sciureus*: three-dimensional architecture, visual screening, and relationships to the neuronal layers. *J Comp Neurol*. 1990;297(1):145–63.
- Minvielle W, Caillaux V, Cohen SY, Chasset F, Zambrowski O, Miere A, Souied EH. Macular microangiopathy in sickle cell disease using optical coherence tomography angiography. *Am J Ophthalmol*. 2016;164:137–144.e31.
- Mitchell P, Smith W, Chey T, Wang JJ, Chang A. Prevalence and associations of epiretinal membranes: the Blue Mountains Eye Study, Australia. *Ophthalmology*. 1997;104(6):1033–40.
- Moriarty B, Acheson R, Condon P, Serjeant G. Patterns of visual loss in untreated sickle cell retinopathy. *Eye*. 1988;2(3):330–5.
- Murakami K, Ho P, Trempe C, Pruett R. Tractional detachment of the macula following branch retinal vein occlusion. *Ann Ophthalmol*. 1983;15(8):760–5.
- Murthy RK, Grover S, Chalam KV. Temporal macular thinning on spectral-domain optical coherence tomography in proliferative sickle cell retinopathy. *Arch Ophthalmol*. 2011;129(2):247–9.
- Network DRCR. Relationship between optical coherence tomography-measured central retinal thickness and visual acuity in diabetic macular edema. *Ophthalmology*. 2007;114(3):525–36.
- Onishi AC, Ashraf M, Soetikno BT, Fawzi AA. Multilevel ischemia in disorganization of the retinal inner layers on projection-resolved optical coherence tomography angiography. *Retina*. 2019;39(8):1588–94.
- Otani T, Kishi S. Correlation between optical coherence tomography and fluorescein angiography findings in diabetic macular edema. *Ophthalmology*. 2007;114(1):104–7.
- Oyster CW. *The human eye*. Sunderland: Sinauer; 1999.
- Park JJ, Soetikno BT, Fawzi AA. Characterization of the middle capillary plexus using optical coherence tomography angiography in healthy and diabetic eyes. *Retina*. 2016;36(11):2039–50.
- Paula KY, Balaratnasingam C, Cringle SJ, McAllister IL, Provis J, Yu D-Y. Microstructure and network organization of the microvasculature in the human macula. *Invest Ophthalmol Vis Sci*. 2010;51(12):6735–43.
- Pecen PE, Smith AG, Ehlers JP. Optical coherence tomography angiography of acute macular neuroretinopathy and paracentral acute middle maculopathy. *JAMA Ophthalmol*. 2015;133(12):1478–80.
- Priluck IA, Buettner H, Robertson DM. Acute macular neuroretinopathy. *Am J Ophthalmol*. 1978;86(6):775–8.



- Rahimy E, Kuehlewein L, Sadda SR, Sarraf D. Paracentral acute middle maculopathy: what we knew then and what we know now. *Retina*. 2015;35:1921.
- Rednam KRV, Jampol LM, Goldberg MF. Scatter retinal photocoagulation for proliferative sickle cell retinopathy. *Am J Ophthalmol*. 1982;93(5):594–9.
- Rispoli M, Savastano MC, Lumbroso B. Capillary network anomalies in branch retinal vein occlusion on optical coherence tomography angiography. *Retina*. 2015;35(11):2332.
- Samara WA, Shahlaee A, Adam MK, Khan MA, Chiang A, Maguire JJ, Hsu J, Ho AC. Quantification of diabetic macular ischemia using optical coherence tomography angiography and its relationship with visual acuity. *Ophthalmology*. 2017;124(2):235–44.
- Sarraf D, Rahimy E, Fawzi AA, Sohn E, Barbazetto I, Zacks DN, Mitra RA, Klancnik JM, Mrejen S, Goldberg NR. Paracentral acute middle maculopathy: a new variant of acute macular neuroretinopathy associated with retinal capillary ischemia. *JAMA Ophthalmol*. 2013;131(10):1275–87.
- Scarinci F, Nesper PL, Fawzi AA. Deep retinal capillary nonperfusion is associated with photoreceptor disruption in diabetic macular ischemia. *Am J Ophthalmol*. 2016;168:129–38.
- Sridhar J, Shahlaee A, Rahimy E, Hong BK, Khan MA, Maguire JJ, Dunn JP, Mehta S, Ho AC. Optical coherence tomography angiography and en face optical coherence tomography features of paracentral acute middle maculopathy. *Am J Ophthalmol*. 2015;160(6):1259–1268.e52.
- Sun JK, Lin MM, Lammer J, Prager S, Sarangi R, Silva PS, Aiello LP. Disorganization of the retinal inner layers as a predictor of visual acuity in eyes with center-involved diabetic macular edema. *JAMA Ophthalmol*. 2014;132(11):1309–16.
- Suzuki N, Hirano Y, Yoshida M, Tomiyasu T, Uemura A, Yasukawa T, Ogura Y. Microvascular abnormalities on optical coherence tomography angiography in macular edema associated with branch retinal vein occlusion. *Am J Ophthalmol*. 2016;161:126–132.e21.
- Weinhaus RS, Burke JM, Delori FC, Snodderly DM. Comparison of fluorescein angiography with microvascular anatomy of macaque retinas. *Exp Eye Res*. 1995;61(1):1–16.
- Wilkinson C, Ferris FL, Klein RE, Lee PP, Agardh CD, Davis M, Dills D, Kampik A, Pararajasegaram R, Verdaguer JT. Proposed international clinical diabetic retinopathy and diabetic macular edema disease severity scales. *Ophthalmology*. 2003;110(9):1677–82.
- Witkin AJ, Rogers AH, Ko TH, Fujimoto JG, Schuman JS, Duker JS. Optical coherence tomography demonstration of macular infarction in sickle cell retinopathy. *Arch Ophthalmol*. 2006;124(5):746–7.
- Yu S, Pang CE, Gong Y, Freund KB, Yannuzzi LA, Rahimy E, Lujan BJ, Tabandeh H, Cooney MJ, Sarraf D. The spectrum of superficial and deep capillary ischemia in retinal artery occlusion. *Am J Ophthalmol*. 2015;159(1):53–63.e52.